RESULTS OF ELECTRON COOLING BEAM STUDIES AT COSY*

C. Böhme, J. Dietrich, V. Kamerdzhiev#, FZJ, Jülich, Germany
M. Bryzgunov, V. Reva, BINP SB RAS, Novosibirsk, Russia
A. Kobets‡, I. Meshkov, A. Rudakov, N. Shurkhno, A. Sidorin, JINR, Dubna, Russia

Abstract

Beam studies dedicated to electron cooling and related problems were carried out at COSY in April 2010. The newly installed Ionization Profile Monitor was used to study the dynamics of longitudinal and transverse electron cooling. Friction force measurements were performed. Beam lifetime was measured for different injection parameters, electron currents and working points. Position and angle scans of the electron beam were also performed. Results of the recent beam studies are reported and the plans for future studies are discussed.

INTRODUCTION

The work was performed under the Helmholtz-Russia Joint Research Group (HRJRG) - HRJRG-106 "Development of a high energy electron cooler for hadron physics experiments at COSY and HESR". A long tradition of cooperation exists with the Budker Institut of Nucler Physics, Novosibirsk and the JINR Dubna in performing experiments at the low energy electron cooler at COSY Jülich.

The electron cooler was designed and constructed during the years 1989 through 1992. The design goal was a 4 A electron beam at 100 keV confined and guided in solenoidal magnetic field up to 0.15 T. Since the first cooling on May 1993 the cooler was mostly operated at injection energy of COSY, which corresponds to electron beam energy of 20 to 25 keV. Practically, electron currents up to 0.5 A are applied. Until recently the solenoid field was set to 0.08 T.

COSY INJECTION SCHEME

In this section, some of the operational features of the stripping injection into COSY are considered, see fig. 1 [1]. The stripper foil is located behind a dipole in the extraction arc, about 40 mm off the nominal orbit. For injection the COSY orbit is bumped to the edge of the foil so that it meets the incoming cyclotron beam position and direction. The injection is controlled by three main parameters, the macropulse length t_{macro}, the bumper ramp down time t_{ramp}, and the micropulsing factor f_{micro}. Controlled by a shutter at the cyclotron, H^- (or D^-) ions are delivered within a time interval t_{macro}. The orbit bumpers are de-energized in the same time. If requested, the cyclotron current I_{cycl} can be decreased by micropulsing, $f_{micro} = 1$ corresponds to 100% I_{cycl}. As injection proceeds, the betatron amplitude of the stored beam increases up to a value determined by the available horizontal acceptance. Multiscattering due to many repeated traversals through the foil and a possible mismatch of incoming and circulating beam angles with subsequent filamentation broaden the stored beam also vertically up to the available acceptance. With the standard values $t_{macro} = t_{ramp} = 20$ ms, no micropulsing, and typically 6 μA cyclotron current, the ring is filled with $(5 – 10)\cdot10^{10}$ protons, but at the expense of large emittances. Based on the aperture of the beam tubes, the optical functions, and the orbit distortions in COSY we estimate acceptances of $A_x = 80$ μm and $A_y = 20$ μm. The proton beam size (3σ emittances) is then larger than the electron beam diameter. If the macropulse is made shorter at constant ramp down time one may expect a beam with smaller emittance but also less stored beam intensity.

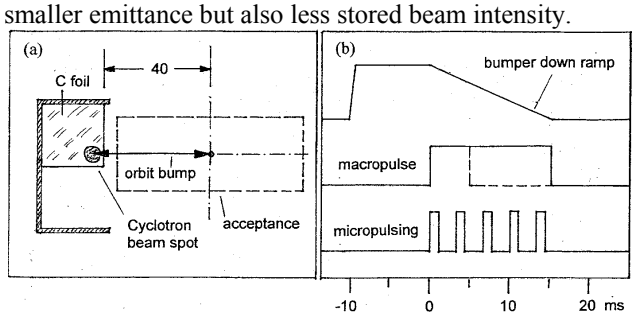

Figure 1: Principle of the stripping injection at COSY. H^- or D^- delivered by the cyclotron injector change their charge state in a carbon foil. Before injection the COSY orbit is bumped to the edge of the stripper foil (a). During the injection time, defined by the macropulse length, the orbit is moving back to its nominal position, coasting beam injection. Bumper ramp down time t_{ramp} and macropulse length t_{macro} are variable parameters (b). Micropulsing by chopping the macropulse allows to reduce the intensity I_{cycl} of the incoming cyclotron beam.

BEAM INSTRUMENTATION

Ionization Profile Monitor

The Ionization Profile Monitor (IPM), developed at GSI [2], is intended to provide fast and reliable non-destructive beam profile measurements at the future FAIR machines. The IPM was installed in COSY to test its performance and reliability and to provide routine non-destructive profile data for COSY.

The ionisation products are guided to a position sensitive detector by transverse electric field. An arrangement consisting of an MCP stack (100x48 mm^2), a luminescent screen, and a 656×494 pixel CCD camera is used to detect ions. High voltage electrodes provide the electric field for ion extraction. The IPM contains two identical units to provide simultaneous measurements in

*Work supported by HRJRG-106
#v.kamerdzhiev@fz-juelich.de
‡ Institute of Electrophysics and Radiation Technologies, Ukraine

both horizontal and vertical planes. The IPM is installed in the arc downstream of the cooler telescope. The data acquisition software described below was developed at COSY (see fig. 2).

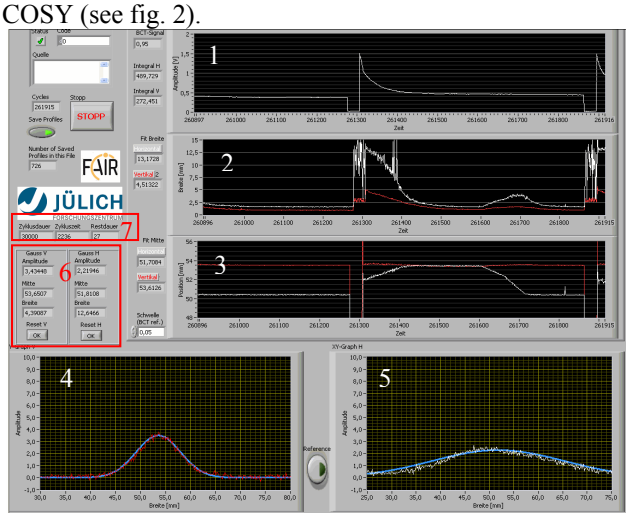

Figure 2: Display of the IPM data acquisition program. Beam Current Transformer (BCT) signal plotted over time (1); horizontal and vertical profile width (Gaussian standard deviation) (2); horizontal and vertical beam position (3); measured vertical beam profile and the corresponding fit (4); measured horizontal beam profile and the corresponding fit (5); summary of vertical and horizontal fit parameters (6); parameters of the current machine cycle (7). The data displayed in 2 and 3 is derived from the corresponding fits. The horizontal axis in 1, 2, 3 represents measurement points. The data acquisition operates at 24 profiles/s. The horizontal axis in 4 and 5 is calibrated in mm. All fits are Gaussian fits.

Beam Current Transformer

The BCT is commercially available from BERGOZ Instrumentation and is based on the CERN design of the Parametric Current Transformer [3, 4]. At injection energy at f_{rev} = 488 kHz, 10 μA of beam current corresponding to $1{,}28 \cdot 10^8$ protons circulating in the ring result in 1 mV at the BCT output.

EXPERIMENTAL RESULTS

Injection optimization

Prior to performing the experiments on electron cooled proton beam, injection parameters were optimized. The current in the last steering magnet of the injection beam line was varied to check for optimal injection angle from the point of view of injection efficiency and proton accumulation. For cooling experiments, injection timing was changed to minimize initial losses [5] at the very beginning of the machine cycle. Injection duration was reduced to t_{macro}= 2 ms instead of standard t_{macro}= 20 ms insuring smaller horizontal emittance of the injected proton beam and thus less beam loss. Injection delay of 5 ms was found to result in the highest injected proton current. Fig. 3 shows the proton current vs. injection delay at t_{macro}= 2 ms. The delay of 5 ms is clearly the preferred value. Fig. 4 shows the time evolution of horizontal beam profiles in a 2.5 s cycle as contour plots for three different injection delay values.

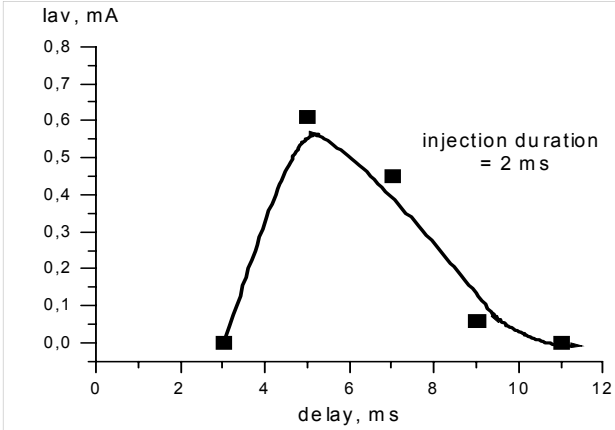

Figure 3: Injected proton current vs injection delay at t_{macro}= 2 ms.

The values 7 ms and 9 ms clearly result in double-peak profiles due to large betatron amplitudes of the injected protons.

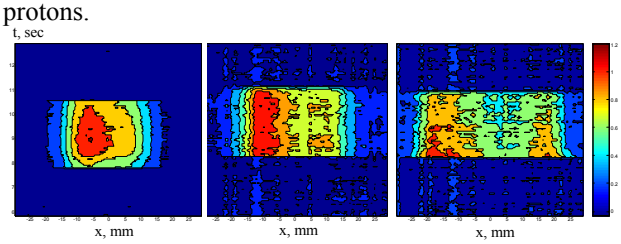

Figure 4: Contour plots representing the evolution in time of the horizontal profiles at different delay time values (5, 7 and 9 ms) at t_{macro}= 2 ms.

The majority of the further experiments were performed with the following injection settings: injection steerer magnet at 20% of maximum current, injection delay 5 ms and t_{macro}= 2 ms. Furthermore, the orbit was kept unchanged to ensure the reproducibility of the measurements. The latest experimental studies which are not described in this report show that significant improvement of beam lifetime can be achieved through orbit optimization. For the experiments reported here some standard cooling orbit was used, thus relative changes of lifetime are of interest rather than absolute values.

Proton beam lifetime and cooling time vs. electron beam position and angle

Preliminary studies of the dependence of proton beam lifetime on the angle between proton and electron beams and the position of the electron beam in respect to the proton beam were performed. The angle scan revealed no strong dependence of beam lifetime on angle within a few seconds after injection. The parallel shift of the electron beam $\Delta x = \Delta y$ =4.5 mm resulted in lifetime improvement by about a factor of 2 (see fig. 5). This, likely, means that in the initial configuration the closed orbit did not pass through the center of the electron beam.

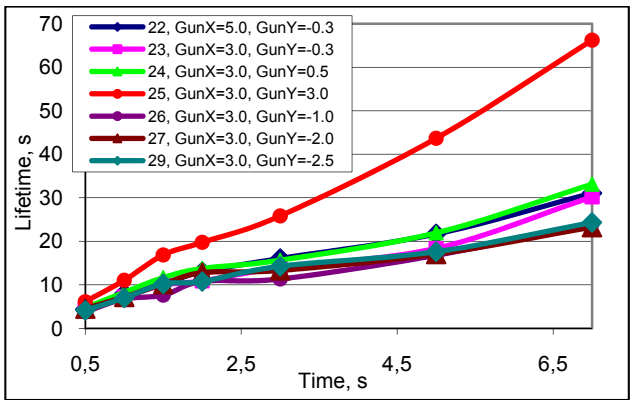

Figure 5: Instantaneous beam lifetime vs. time for different electron beam positions. The e-beam position was varied by adjusting the currents in the gun and collector corrector coils. 3 A correspond to a position change of 4.5 mm in the cooling section. $Q_x \approx Q_y \approx 3.61$.

A full scan with the electron beam across the proton beam could not be performed due to limitations in the cooler systems. These studies need to be repeated by moving the electron beam across the cooled proton beam and vice versa.

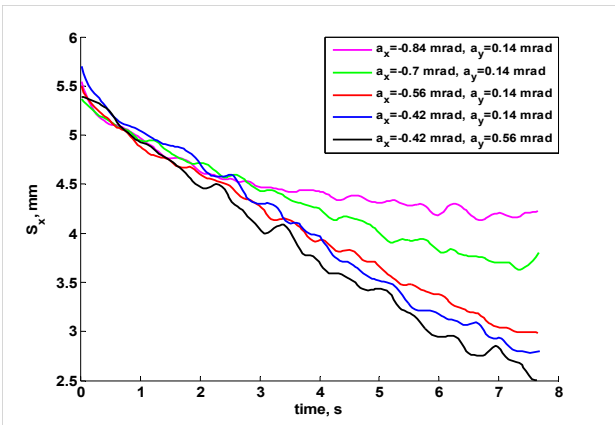

Figure 6: Proton horizontal beam width (Gaussian standard deviation) for different angles of electron beam.

During the angle scan beam profiles measured by the IPM were recorded. Result of the analysis is shown in fig. 6. Plotted is the width of the horizontal profile over time. Though there is no significant change of lifetime, an effect on cooling time was observed. After about 3 s the rate of width decrease begins to change for angles $a_x < -0.5$ mrad. This may be due to the higher effective electron temperature which begins to matter once protons have been cooled to some extent.

Varying the electron beam angle in respect to the proton beam can be used to control the beam emittance. This was done recently during the beam studies dedicated to beam lifetime optimization for PAX experiment [6].

Proton beam lifetime vs. electron current

Dependence of proton beam lifetime on electron beam current is shown in fig. 7. It was measured at optimal electron beam position and angle. If we consider the long-term lifetime, the electron current has an optimum around 110 mA. However, much higher current (290 mA) results in better lifetime on a basis of a few tens of seconds. Finally, the short-term lifetime, few seconds after injection, drops with growing electron current, being the best with no electron current at all – initial losses [5, 6]. Poor long-term lifetime at higher electron currents can be explained by the interplay of single scattering of protons on residual gas and non-linear electric field of the electron beam.

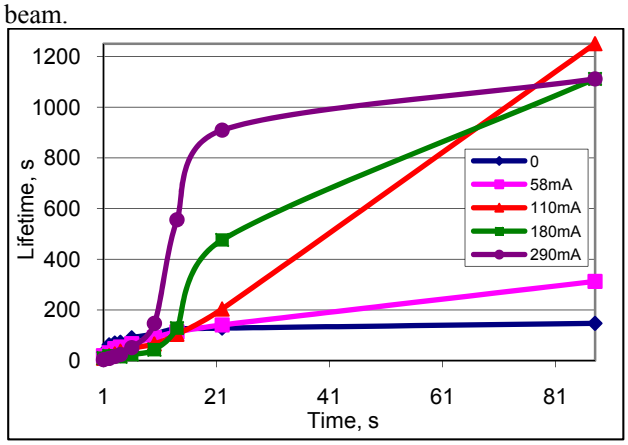

Figure 7: Variation of instantaneous beam lifetime during first 90 s for different electron currents.

Dependence of proton beam lifetime on tunes

Dependence of beam lifetime on the working point during electron cooling was measured. Although the lifetime changes fast as the cooling proceeds the change of tunes results in a change of lifetime in all timescales. The setting $Q_x \approx Q_y \approx 3.61$ was found to provide good lifetime and was used for the experiments. However, we have seen evidence that the values aside from the resonance line e.g. $Q_x \approx 3.613$, $Q_y \approx 3.607$ or $Q_x \approx 3.608$, $Q_y \approx 3.616$ may be suitable as well.

Friction force measurements

The presence of dispersion at the IPM location can be very helpful for resolving small energy changes. This technique was used to estimate the mean value of the longitudinal friction force by introducing a step to the electron acceleration voltage (see fig 8).

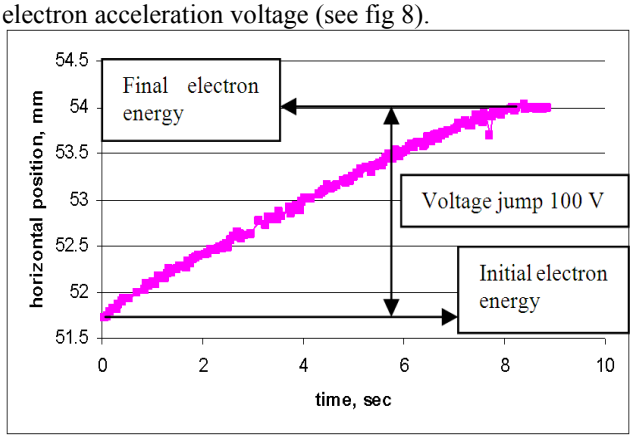

Figure 8: Change of proton beam position, as measured by the IPM, in response to the change of electron energy by 100 eV.

$$\langle F \rangle = \frac{2CE\Delta x}{l_e D \beta c \Delta t} \approx 1.9 \cdot 10^{-4} \frac{eV}{cm} \quad (1)$$

Where $E = 45\ MeV$ is the ion kinetic energy, $C = 184\ m$ the machine circumference, $l_e \approx 1.4\ m$ the effective length of the cooling section, $D = 2\ m$ dispersion at the IPM location, $\beta c = 8.97 \cdot 10^7\ m/s$, $\Delta x \approx 2.25\ mm$ the horizontal displacement at the IPM and $\Delta t \approx 8\ s$ time required to reach the new energy. This value agrees well with previous measurements based on revolution frequency shift as a result of an electron energy step.

Transverse friction force can be determined by analyzing the evolution of beam profiles during the cooling process. The experimental values of the distribution function enable to calculate the time derivative and to estimate the friction force according to equation

$$F(a_n) = \frac{1}{f(a_n)} \sum_{i=1}^{n} \frac{\Delta f_i}{\Delta t} \Delta a \quad (2)$$

where f is the proton distribution function, F is an effective friction force, a is the amplitude of betatron oscillation. The profile of the friction force can be approximated by phenomenological equation

$$F(a) = \frac{A \cdot a_{eff}^2 \cdot a}{\left(a^2 + a_{eff}^2\right)^{3/2}} \quad (3)$$

and the typical cooling rate $\lambda = dF(a)/da$ can be calculated at the point $a = 0$. Fig. 9 shows the curves of the friction force estimated according to equation (2) and the approximation curve (3). The electron current and acceleration voltage were set to 180 mA and 24.58 kV respectively. Fig. 10 shows the dependence of cooling rate on the value of electron beam current. Evidently, the maximum cooling rate of 0.25 sec^{-1} corresponds to electron current of about 300 mA.

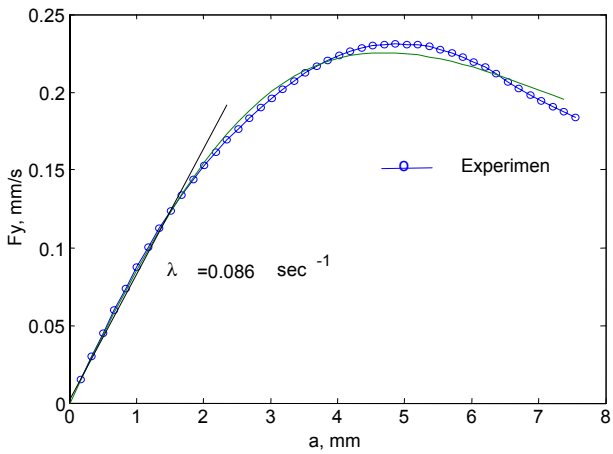

Figure 9: Experimental friction force curve (circles) according to (2) and an approximation according to (3) (solid line). The cooling rate at $a = 0$ is $\lambda = dF(a)/da$ =0.086 sec^{-1}.

Interestingly, once the final proton beam size is reached $\sigma_v \approx 1$ mm with electron currents above 100 mA, further increase of electron current does not result in a decrease of the proton beam size (see fig. 11). This observation does not seem to be related to the ability of the IPM to resolve small beam size. Vertical beam size of low intensity proton beam equal to 0.67 mm has been measured before.

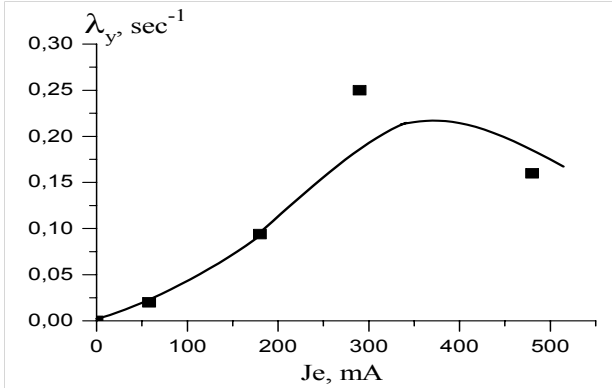

Figure 10: Dependence of cooling rate on electron current.

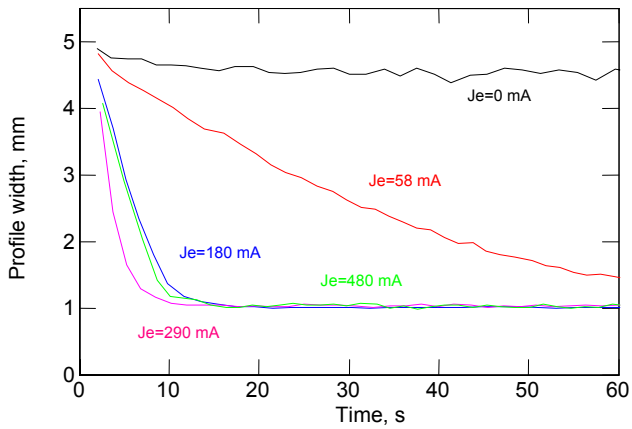

Figure 11: Evolution of the vertical beam size in time for different values of electron current.

Fig. 12 shows time evolution of the horizontal and vertical beam widths. Four regions are marked on the plot. The proton beam is injected at t ≈ 0 s. The initial cooling with 170 mA of electron current is shown in the first region. This process is accompanied by initial losses, so the reduction of beam width is a result of cooling and beam loss. After the beam has reached equilibrium at t ≈ 30 s electron current was turned off allowing the beam size to grow (region 2). After another 30 s electron current is turned on again, leading to fast decrease of beam size (region 3). In the fourth region emittance blow-up without electron cooling is shown again. No beam losses have been observed after 10 s, corresponding to regions 2-4. An exponential fit $y = y_0 + \exp(-(t-t_0)/\tau)$ was performed in region 3 corresponding to beam cooling. In region 4 exponential and linear fits were done. Exponential beam blow up is mostly due to intrabeam scattering, whereas the linear one is due to interaction of the beam with residual gas. Significantly different slope of linear growth can be explained by the difference of mean beta functions in the ring. Fig. 13 shows three profile snapshots for the cooling-heating process indicated in fig. 12.

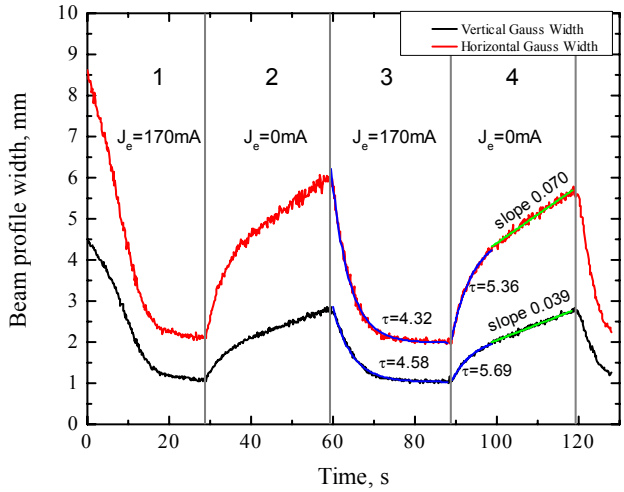

Figure 12: Horizontal and vertical beam width (Gaussian standard deviation) plotted vs. time with electron cooling on and off. Beam intensity after initial losses amounted to about $5 \cdot 10^9$ protons, average vacuum in COSY was about 10^{-9} mbar. Profile snapshots are shown in fig. 13.

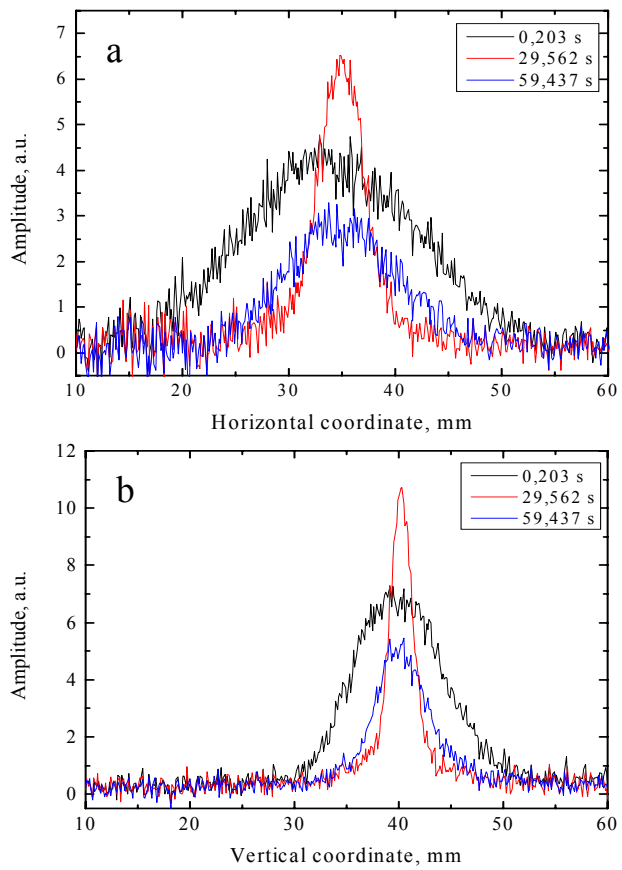

Figure 13: Horizontal (a) and vertical (b) beam profiles after injection (0.2 s), at equilibrium after cooling (29.5 s) and after 30 s without cooling (59.4 s). Continuous evolution of beam width is shown in fig. 12.

CONCLUSIONS

The dependence of cooling efficiency and proton beam lifetime on electron beam position and angle was studied. Beam lifetime does not appear to be sensitive to the electron beam angle in presence of cooling, even though the cooling force may drop significantly and equilibrium beam size become larger. Parallel displacement of electron beam courses more effect on beam lifetime. There is one optimal position, corresponding to coaxial alignment of two beams resulting in best lifetime. The expected significant losses in the case of proton beam being at the edge of the electron beam could not be observed, partly due to limitations of electron beam positioning. This experiment needs to be performed by moving the proton beam across the electron one and vice versa. The longitudinal cooling force was estimated by detecting the change of horizontal beam position at the IPM location in response to the change of electron energy. Dependence of transverse cooling force on electron beam current was studied. The value 300 mA was found to correspond to the maximum cooling force. The short-term lifetime drops with increase of electron current supporting the explanation of initial losses offered in [5, 7]. Mid-term lifetime improves with higher electron current, whereas the long-term one has maximum at about 110 mA. This can qualitatively be explained by the beam interaction with residual gas in conjunction with non-linear field of the electron beam. The optimal working point was found for the orbit used. However, during the tune scan the orbit was not controlled. For future cooling studies more attention should be paid to orbit smoothing, using the orbit optimization techniques that recently became available at COSY. The IPM performed well and delivered very useful data. Additional functionality of the data analysis software is under discussion. Online friction force calculation would make electron cooler adjustment easier. Profile fitting with a sum of Lorentz and Gauss distributions has been proposed to improve fit accuracy.

ACKNOWLEDGEMENTS

The authors greatly appreciate the help and advice of their colleagues R. Gebel, B. Lorentz, D. Prasuhn, K. Reimers, R. Stassen, H.J. Stein of the IKP, FZJ and V. Parkhomchuk of the BINP, Novosibirsk.

REFERENCES

[1] H. J. Stein et al., Present Performance of Electron Cooling at COSY-Jülich, Proceedings RuPAC2002.
[2] T. Giacomini et al., Development of Residual Gas Profile Monitors at GSI, Proceedings BIW04.
[3] K.B. Unser, "Beam current transformer with DC to 200 MHz range," IEEE Trans. Nucl. Sci., NS-16, June 1969, pp. 934-938.
[4] BERGOZ Instrumentation.
[5] A. Kobets et al., Loss Phenomena of Electron Cooled Ion Beams, IKP Annual Report 2006.
[6] PAX Collaboration, Technical Proposal for Antiproton–Proton Scattering Experiments with Polarization, http://arxiv.org/abs/hep-ex/0505054.
[7] Yu. Senichev et al., Electron Cooled Beam Losses Phenomena in COSY, Proceedings HB2010.